

# New Temperature Measurements in $^{197}\text{Au} + ^{197}\text{Au}$ Collisions

W. Trautmann<sup>(1)</sup> for the ALADIN collaboration:

R. Bassini,<sup>(2)</sup> M. Begemann-Blaich,<sup>(1)</sup> A.S. Botvina,<sup>(3)\*</sup> S. Fritz,<sup>(1)</sup> S.J. Gaff,<sup>(4)</sup>  
C. Groß,<sup>(1)</sup> G. Immé,<sup>(5)</sup> I. Iori,<sup>(2)</sup> U. Kleinevoß,<sup>(1)</sup> G.J. Kunde,<sup>(4)</sup> W.D. Kunze,<sup>(1)</sup>  
U. Lynen,<sup>(1)</sup> V. Maddalena,<sup>(5)</sup> M. Mahi,<sup>(1)</sup> T. Möhlenkamp,<sup>(6)</sup> A. Moroni,<sup>(2)</sup>  
W.F.J. Müller,<sup>(1)</sup> C. Nociforo,<sup>(5)</sup> B. Ocker,<sup>(7)</sup> T. Odeh,<sup>(1)</sup> F. Petruzzelli,<sup>(2)</sup>  
J. Pochodzalla,<sup>(1)†</sup> G. Raciti,<sup>(5)</sup> G. Riccobene,<sup>(5)</sup> F.P. Romano,<sup>(5)</sup> Th. Rubehn,<sup>(1)‡</sup>  
A. Saija,<sup>(5)</sup> M. Schnittker,<sup>(1)</sup> A. Schüttauf,<sup>(7)</sup> C. Schwarz,<sup>(1)</sup> W. Seidel,<sup>(6)</sup>  
V. Serfling,<sup>(1)</sup> C. Sfienti,<sup>(5)</sup> A. Trzcinski,<sup>(8)</sup> G. Verde,<sup>(5)</sup> A. Wörner,<sup>(1)</sup> Hongfei Xi,<sup>(1)§</sup>  
and B. Zwieglinski<sup>(8)</sup>

<sup>(1)</sup>Gesellschaft für Schwerionenforschung, D-64291 Darmstadt, Germany

<sup>(2)</sup>Istituto di Scienze Fisiche dell' Università and I.N.F.N., I-20133 Milano, Italy

<sup>(3)</sup>Institute for Nuclear Research, Russian Academy of Sciences, 117312 Moscow ,  
Russia

<sup>(4)</sup>Department of Physics and Astronomy and National Superconducting Cyclotron  
Laboratory, Michigan State University, East Lansing, MI 48824, USA

<sup>(5)</sup>Dipartimento di Fisica dell' Università and I.N.F.N., I-95129 Catania, Italy

<sup>(6)</sup>Forschungszentrum Rossendorf, D-01314 Dresden, Germany

<sup>(7)</sup>Institut für Kernphysik, Universität Frankfurt, D-60486 Frankfurt, Germany

<sup>(8)</sup>Soltan Institute for Nuclear Studies, 00-681 Warsaw, Hoza 69, Poland

## ABSTRACT

We report on new measurements of breakup temperatures for target spectators from  $^{197}\text{Au} + ^{197}\text{Au}$  reactions at 1000 MeV per nucleon. The temperatures rise with decreasing impact parameter from 4 MeV for peripheral to about 10 MeV for the most central collisions, in good agreement with previous results for projectile spectators at 600 MeV per nucleon.

The measured temperatures agree quantitatively with the breakup temperatures predicted by the statistical multifragmentation model. For these calculations a relation between the initial excitation energy and mass was derived which gives good simultaneous agreement for the fragment charge correlations.

---

\* Present Address: Bereich Theoretische Physik, Hahn-Meitner-Institut, D-14109 Berlin, Germany

† Present address: Max-Planck-Institut für Kernphysik, D-69117 Heidelberg, Germany

‡ Present address: Nuclear Science Division, Lawrence Berkeley Laboratory, Berkeley, CA 94720, USA

§ Present address: NSCL, Michigan State University, East Lansing, MI 48824, USA

The energy spectra of light charged particles and the behaviour of the mean kinetic energies of neutrons indicate a substantial component of light particle emission prior to the final breakup stage.

# 1 Introduction

The correlated measurements of the nuclear temperature and the excitation energy for excited projectile spectators in  $^{197}\text{Au} + ^{197}\text{Au}$  collisions at 600 MeV per nucleon has permitted to extend the caloric curve of nuclei to very high excitation energies, far beyond the nuclear binding energy [1, 2]. For the temperature determination the method suggested by Albergo *et al.* has been used which is based on the assumption of chemical equilibrium and requires the measurement of double ratios of isotopic yields [3]. The obtained temperatures, plotted against the measured excitation energy, resulted in a caloric curve with the characteristic behavior reminiscent of first-order phase transitions in macroscopic systems. The 'liquid' and the 'vapor' regimes where the temperature rises with increasing excitation energy are separated by a region of nearly constant temperature  $T \approx 5$  MeV over which the multiplicity of the fragmentation products increases.

The present discussion of the caloric curve mainly centers around three points. The first one concerns the methodical question of whether breakup temperatures can be reliably deduced from isotopic yield ratios in the presence of sequential-decay processes by which these ratios may be modified after the breakup has occurred [4, 5]. Model calculations show that the amount of modification depends on the breakup density which is not very well known [2,6-8]. The potential directions of interpretation, in a wider sense, of these new experimental results constitute the second topic of discussion [9-11]. Finally, there is numerous work concerned with the consequences for finite nuclei [12, 13] of the predicted first-order phase transition in nuclear matter [14, 15] (for very recent references see, e.g., refs. [16, 17]). In addition, experimental caloric curves for other systems have been reported recently [18, 19].

In this contribution, we present results of new measurements of the breakup temperature in the  $^{197}\text{Au} + ^{197}\text{Au}$  reaction. In particular, we will address two specific questions connected with the statistical interpretation of multi-fragment decays of excited spectator systems: Do the measured temperatures exhibit the same invariance with respect to the entrance channel that has been found for the fragmentation patterns? This universal feature of the spectator decay has become evident in the observed  $Z_{bound}$  scaling of the fragment multiplicities and charge correlations [20]. Here  $Z_{bound}$ , defined as the sum of the atomic numbers  $Z_i$  of all spectator fragments with  $Z_i \geq 2$ , is a quantity closely correlated with the excitation energy transferred during the initial stages of the reaction. Secondly, how do the extracted temperatures compare with the predictions of the statistical multifragmentation model [13] which has been so successful in describing the multiplicities and charge correlations characterizing the universal partition space [21]?

## 2 Experimental method and results

The experiment was performed at the ALADIN spectrometer [20] of the GSI facility with beams of  $^{197}\text{Au}$  of 1000 MeV per nucleon incident energy, provided by the heavy-ion synchrotron SIS. The present data were taken as part of a larger experiment which incorporated three multi-detector hodoscopes for coincident particle detection [8, 22].

A set of seven telescopes, each consisting of three Si detectors with thickness 50, 300, and 1000  $\mu\text{m}$  and of a 4-cm long CsI(Tl) scintillator with photodiode readout, were used to measure the isotopic yields of light charged particles and fragments. Four telescopes were placed in the forward hemisphere while three telescopes were placed at  $\theta_{lab} = 110^\circ$ ,  $130^\circ$ , and  $150^\circ$  for detecting the products of the target-spectator decay. Isotopes in the range from hydrogen to carbon were satisfactorily resolved. Because of the presumably different shapes of  $^3\text{He}$  and  $^4\text{He}$  spectra at low energies, a correction was required in order to compensate for the effect of the detection threshold  $E \approx 12$  MeV for helium ions, resulting from triggering with the 300- $\mu\text{m}$  detector. For a global characterization of the reaction and impact parameter selection, the quantity  $Z_{bound}$  of the coincident projectile decay was measured with the time-of-flight (TOF) wall of the ALADIN spectrometer.

Emission temperatures  $T$  were deduced from the double ratios  $R$  formed by combining the ratio of  $^3\text{He}/^4\text{He}$  yields with either the lithium yield ratio  $^6\text{Li}/^7\text{Li}$  or with the hydrogen yield ratios p/d or d/t. The set of  $^3\text{He}$ ,  $^4\text{He}$ ,  $^6\text{Li}$ , and  $^7\text{Li}$  isotopes is the one used previously for the determination of breakup temperatures of projectile spectators in  $^{197}\text{Au} + ^{197}\text{Au}$  at 600 MeV per nucleon [1, 2]. Combinations involving p, d, or t, together with  $^3\text{He}$  and  $^4\text{He}$ , have the advantage of larger production cross sections, particularly in the 'vapor' regime where the heavier fragments are becoming rare. The three expressions are

$$T_{\text{HeLi},0} = 13.3 / \ln\left(2.2 \frac{Y_{^6\text{Li}}/Y_{^7\text{Li}}}{Y_{^3\text{He}}/Y_{^4\text{He}}}\right) \quad (1)$$

and

$$T_{\text{Hepd},0} = 18.4 / \ln\left(5.6 \frac{Y_{^1\text{H}}/Y_{^2\text{H}}}{Y_{^3\text{He}}/Y_{^4\text{He}}}\right) \quad (2)$$

and

$$T_{\text{Hedt},0} = 14.3 / \ln\left(1.6 \frac{Y_{^2\text{H}}/Y_{^3\text{H}}}{Y_{^3\text{He}}/Y_{^4\text{He}}}\right) \quad (3)$$

where the temperatures are given in units of MeV.

The subscript 0 is meant to indicate that these apparent temperatures, derived from the measured ground-state populations, may be affected by feeding of these populations from sequentially decaying excited states. The required corrections were calculated with the quantum statistical model which starts from chemical equilibrium at a given temperature, density, and neutron-to-proton (N/Z) ratio and which

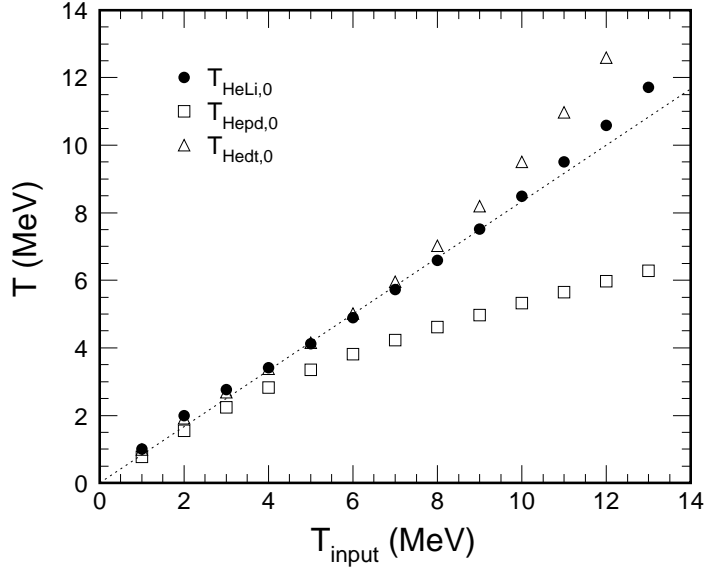


Figure 1: Apparent temperatures  $T_{HeLi,0}$ ,  $T_{Hepd,0}$ , and  $T_{Hedt,0}$ , according to the quantum statistical model, as a function of the input temperature  $T_{input}$ . A breakup density  $\rho/\rho_0 = 0.3$  is assumed. The dotted line represents the linear relation  $T_0 = T_{input}/1.2$ .

includes sequential decay [23, 24]. In Fig. 1, the three apparent temperatures defined in eqs. (1-3) are shown as a function of the equilibrium temperature  $T_{input}$  for the parameters  $N/Z = 1.49$  (value of  $^{197}\text{Au}$ ) and density  $\rho = 0.3 \cdot \rho_0$  (where  $\rho_0$  is the saturation density of nuclei). The relations between  $T_{HeLi,0}$  or  $T_{Hedt,0}$  and  $T_{input}$  are almost linear and the corrections required in these two cases are practically identical, except at the highest temperatures. The linear approximation, indicated by the dotted line, corresponds to the constant correction factor  $T = 1.2 \cdot T_0$  adopted for  $T_{HeLi}$  in Ref. [1]. Apparently,  $T_{Hepd,0}$  is more strongly affected by feeding effects at the higher temperatures. Within the range of densities  $0.1 \leq \rho/\rho_0 \leq 0.5$ , the corrections required according to the quantum statistical model vary within about  $\pm 15\%$  [2, 25]. They virtually do not change with the  $N/Z$  ratio of the primary source. In the analysis, the corrections calculated for  $\rho/\rho_0 = 0.3$ , as derived from the results shown in Fig. 1, were applied.

In Fig. 2 the obtained temperatures  $T_{HeLi}$ ,  $T_{Hepd}$ , and  $T_{Hedt}$  are shown as a function of  $Z_{bound}$ . They are based on the yield ratios measured with the telescope at the most backward angle  $\theta_{lab} = 150^\circ$ . Simulations indicate that, at this angle, contributions from the midrapidity source are negligible. The temperatures increase continuously with decreasing  $Z_{bound}$  from  $T = 4$  MeV for peripheral collisions to about 10 MeV for the most central collisions associated with the smallest  $Z_{bound}$  values. The range  $Z_{bound} \leq 20$  corresponds to the high excitation energies at which

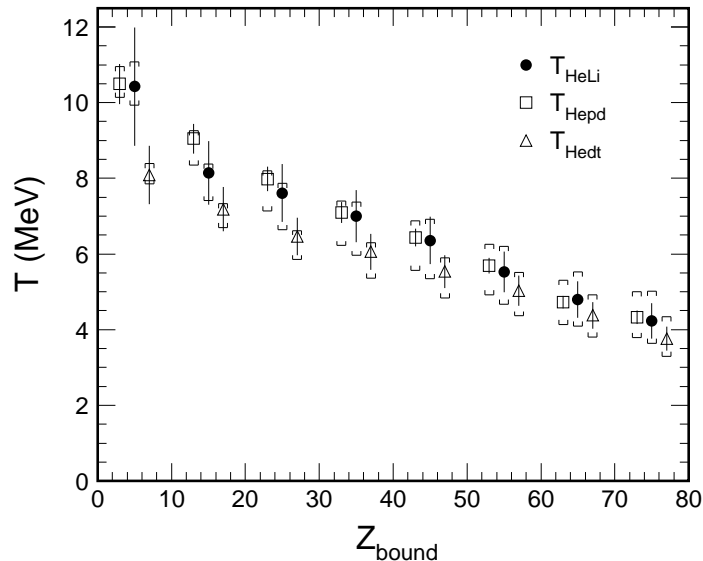


Figure 2: Temperatures  $T_{HeLi}$ ,  $T_{Hepd}$ , and  $T_{Hedt}$  as a function of  $Z_{bound}$ , averaged over bins of 10-units width. Corrections have been applied as described in the text. The error bars represent the statistical uncertainty. The systematic uncertainty, caused by the extrapolation of the yields of helium isotopes below the identification threshold, is indicated by the brackets. For clarity, the open data symbols are laterally displaced by 2 units of  $Z_{bound}$ .

the upbend of the temperature appears in the caloric curve [1]. The results obtained with the three different double ratios agree rather well which is remarkable in view of the different feeding corrections that are required, in particular, in the case of  $T_{Hepd}$ .

### 3 Universality of spectator temperatures

The universality of spectator fragmentation has first been recognized in the study of the charge partitions [20, 26]. Universality, in the present context, refers to the invariance of the fragmentation patterns of excited spectator nuclei with respect to the properties of the entrance channel. The decaying system has lost the memory of how it was formed. This was shown to be valid for the variation of the bombarding energy (beyond about 400 MeV per nucleon) and for the variation of the target mass (if we consider the case of projectile fragmentation). If a linear scaling law is applied, it is even valid for the variation of the projectile mass itself. The search for the deeper symmetries behind these universal properties of the fragment decay is presently pursued by several groups [27, 28].

The data show that the invariance with respect to the entrance channel includes

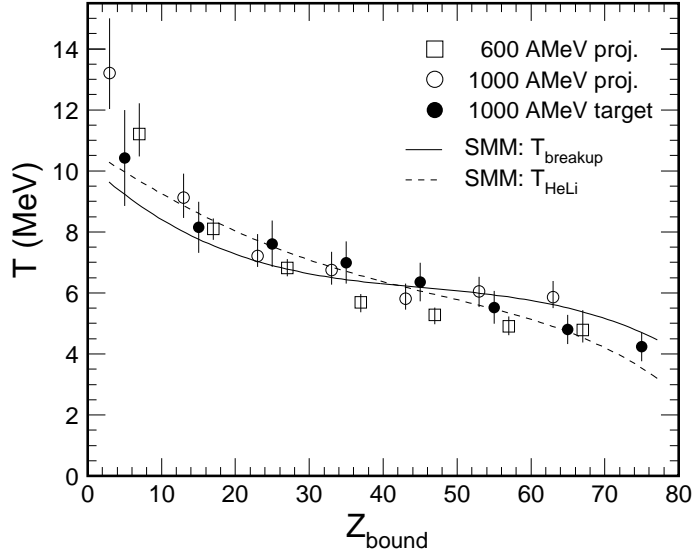


Figure 3: Temperatures  $T_{\text{HeLi}}$  of the target spectator from the present experiment at  $E/A = 1000$  MeV (dots) and of the projectile spectator (from Ref. [25]) at  $E/A = 600$  MeV (open squares) and 1000 MeV (open circles) as a function of  $Z_{bound}$ . The data symbols represent averages over bins of 10-units width. For clarity, the open data symbols are laterally displaced by 2 units of  $Z_{bound}$ . The full and dashed lines represent the breakup temperature  $T_{breakup}$  and the isotopic temperature  $T_{\text{HeLi}}$  calculated with the statistical multifragmentation model.

the deduced isotope temperatures. In Fig. 3 the  $T_{\text{HeLi}}$  temperatures from this work and those derived previously [1, 25, 29] for projectile spectators in  $^{197}\text{Au} + ^{197}\text{Au}$  collisions at 600 and 1000 MeV per nucleon are shown in comparison. In the case of the projectile decays, the isotopes were identified by tracking of their trajectories with the upgraded TP-MUSIC detector and subsequent momentum and time-of-flight analysis. The agreement obtained in the measurements at 1000 MeV per nucleon for the projectile and the target decays, performed with different methods of isotope identification and associated with different detection thresholds, reflects the experimental accuracy. The agreement of the data measured at 600 and 1000 MeV per nucleon confirms the expectation that the breakup temperature, as a function of  $Z_{bound}$ , does not change with the bombarding energy.

Neither does the breakup temperature depend on the mass of the collision partner. In Fig. 4 this is demonstrated for the case of  $^{197}\text{Au}$  projectiles of 600 MeV per nucleon impinging on C, Al, Cu, Au targets. The breakup temperatures deduced by the EOS collaboration for  $^{197}\text{Au} + \text{C}$  at 1 GeV per nucleon [18] are also consistent with this conclusion. Within the range  $Z_{bound} \geq 40$  which is mainly populated in this reaction

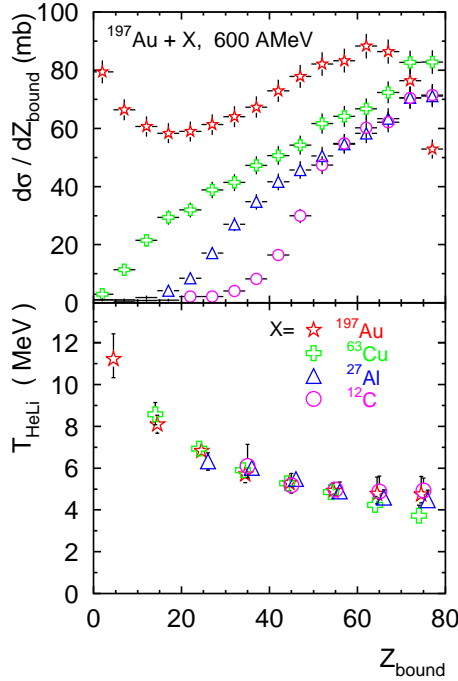


Figure 4: Top: Measured cross sections  $d\sigma/dZ_{bound}$  for the reactions of  $^{197}\text{Au}$  projectiles at  $E/A = 600$  MeV with the four targets C, Al, Cu, and Au. Note that the experimental trigger affected the cross sections for  $Z_{bound} \geq 65$ .

Bottom: Breakup temperature  $T_{\text{HeLi}}$  for the same four reactions (from Ref. [25]).

(Fig. 4, top, and Ref. [20]), they are in good agreement with the present results for  $^{197}\text{Au} + ^{197}\text{Au}$ , both in absolute magnitude and in their dependence on the impact parameter. The observed universality is a strong indication for equilibrium being reached at the breakup stage which is a necessary condition for a statistical description of the fragmentation process.

## 4 Statistical model description

Calculations within the statistical multifragmentation model [13] were performed in order to test its consistency with respect to the statistical parameters and predicted charge partitions. In the model one assumes that all observed particles come from the decay of one equilibrated source.

As a criterion for selecting the distribution in excitation energy and mass of the ensemble of excited spectator nuclei, required as input for the calculations, we chose the capability of the model to simultaneously describe the correlations of the mean multiplicity  $\langle M_{IMF} \rangle$  of intermediate-mass fragments (IMF's) and of the mean charge asymmetry  $\langle a_{12} \rangle$  with  $Z_{bound}$ . The asymmetry  $a_{12}$  of the two largest fragments is



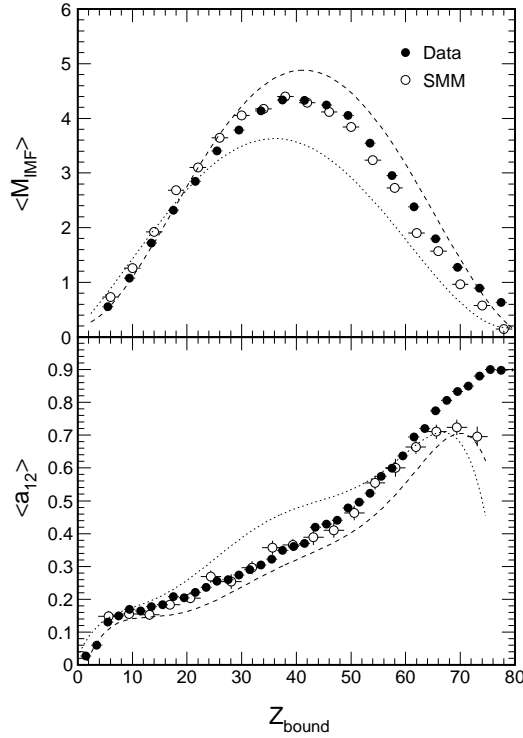


Figure 5: Mean multiplicity of intermediate-mass fragments  $\langle M_{IMF} \rangle$  (top) and mean charge asymmetry  $\langle a_{12} \rangle$  (bottom) as a function of  $Z_{bound}$ , as obtained from the calculations with the statistical multifragmentation model (open circles) in comparison to the experiment (dots, from Ref. [20]). The dashed and dotted lines show the results of the calculations with excitation energies  $E_x/A$  15% above and 15% below the adopted values, respectively. Note that the trigger threshold affected the data of Ref. [20] at  $Z_{bound} \geq 65$ .

defined as  $a_{12} = (Z_{max} - Z_2)/(Z_{max} + Z_2)$ , with the mean value to be calculated from all events with  $Z_{max} \geq Z_2 \geq 2$ . The comparison, shown in Fig. 5, was based on the data reported in Ref. [20]. In the region  $Z_{bound} > 30$  the mean excitation energy of the ensemble of spectator nuclei was found to be well constrained by the mean fragment multiplicity alone. At  $Z_{bound} \approx 30$  and below, the charge asymmetry was a necessary second constraint (cf. Ref. [30]) while, at the lowest values of  $Z_{bound}$ , neither the multiplicity nor the asymmetry provided rigid constraints on the excitation energy. These sensitivities are illustrated in Fig. 5 where the dashed and dotted lines show the model results for  $E_x/A$  chosen 15% above and below the adopted values.

The solid line in Fig. 3 represents the thermodynamical temperature  $T$  obtained from the calculations. Within the given experimental and methodical uncertainties, it is in very good agreement with the data. The description of the fragmentation as a

statistical process is thus internally consistent, the temperatures needed to reproduce the observed partition patterns correspond to those measured. The comparison is even more consistent if we take directly the temperature  $T_{\text{HeLi}}$  that is obtained from the calculated isotope yields and corrected in the same way as the experimental data (dashed line). The agreement of the measured and model  $T_{\text{HeLi}}$  is excellent, and the tendency of being lower (higher) than the thermodynamical temperature at the larger (smaller) values of  $Z_{\text{bound}}$  is common to both. According to the statistical multifragmentation model, therefore, the true source temperature varies only from  $T = 5$  MeV for peripheral to about 9 MeV for the most central collisions and stays rather constant  $T \approx 6$  MeV over a wide range of  $Z_{\text{bound}}$ , i.e. over a wide range of excitation energies, where the maximum production of intermediate-mass fragments is observed.

The excitation energies that have resulted from this procedure are somewhat larger than what was found previously in analyses [21,30-32] of the earlier  $^{197}\text{Au}$  on Cu data at 600 MeV per nucleon [33]. The difference reflects the sensitivity to the fragment multiplicity and is caused by the slightly larger mean multiplicities that were obtained from the more recent experiments with improved acceptance [20]. They are still considerably lower than the energies obtained from the calorimetric measurement of the total energy deposit (see section 6). A (partial) resolution of this discrepancy may come from pre-breakup emission of light particles carrying away energy as the spectator system approaches the final breakup stage.

## 5 Indications of pre-breakup emission

Kinetic energy spectra were studied for light charged particles up to  $^4\text{He}$ . For the five species proton, deuteron, triton,  $^3\text{He}$ , and  $^4\text{He}$ , the spectra measured at  $\theta_{\text{lab}} = 150^\circ$  and integrated over finite regions of  $Z_{\text{bound}}$  are shown in Fig. 6. For comparison, the predictions calculated with the statistical fragmentation model are also given. The two sets of experimental and model spectra are each normalized, and one overall normalization factor is used to relate the two sets. It was adapted to the yields of  $Z = 2$  fragments because their calculated multiplicities, as a function of  $Z_{\text{bound}}$ , are found to satisfactorily reproduce the experimental multiplicities reported in Ref. [20].

The main trend apparent from the comparison is a systematically increasing deviation of the experimental from the model spectra with decreasing  $Z_{\text{bound}}$ , i.e. increasing centrality, and with decreasing particle mass. It not only affects the slope parameters describing the shape of the spectra but also the integrated intensities. The yields of hydrogen isotopes, and in particular of the protons, are grossly underestimated by the statistical multifragmentation model. In the case of  $^4\text{He}$ , on the other hand, the equilibrium description accounts rather well for the multiplicities and kinetic energies. A major contribution to the observed  $^4\text{He}$  yields is expected

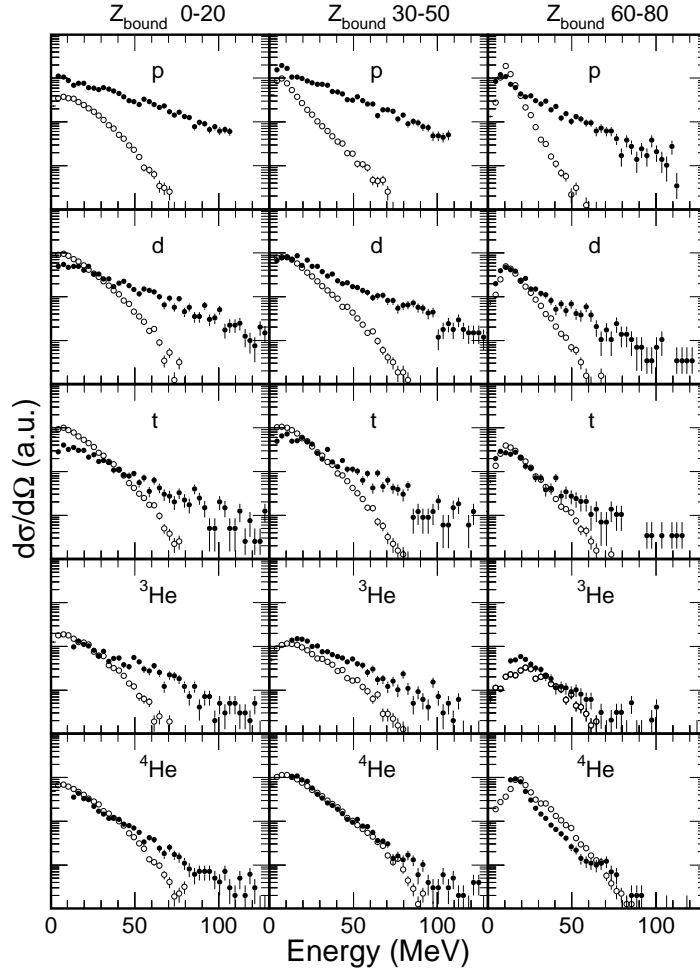


Figure 6: Energy spectra, measured at  $\theta_{\text{lab}} = 150^\circ$ , of light charged particles p, d, t,  ${}^3\text{He}$ , and  ${}^4\text{He}$  for three intervals of  $Z_{\text{bound}}$  as indicated. The dots represent the measured spectra, the open circles are the results of the calculations with the statistical multifragmentation model. The spectra are normalized as stated in the text.

to come from evaporation by large fragments and excited residue-like nuclei which, apparently, is modelled well.

Conceivable mechanisms that cannot explain the observed deviations include collective flow and Coulomb effects which both should act in proportion to the mass or charge of the emitted particle, contrary to what is observed. On the other hand, the commonly adopted scenario of freeze-out after expansion involves a pre-breakup phase during which the system cools not only by adiabatic expansion but also by the emission of light particles, predominantly nucleons but also light complex particles [10, 31, 34]. The spectra should reflect the higher temperatures at the earlier stages

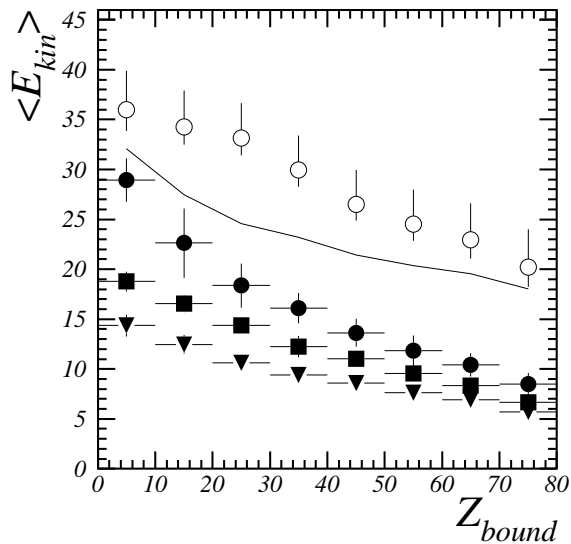


Figure 7: Mean kinetic energy of neutrons (full symbols) in the rest frame of the projectile spectator as obtained in measurements with LAND for the three bombarding energies 600 (triangles), 800 (squares), and 1000 MeV per nucleon (circles). For the case of 1000 MeV per nucleon, a comparison is made between the measured mean kinetic energies of protons (open circles) and those obtained by adding estimated Coulomb contributions to the neutron kinetic energies (full line).

of the reaction, prior to the final breakup into fragments, but not necessarily exhibit a clear preequilibrium character (cf. Ref. [35]).

A significant component of pre-breakup emission in the light particle yields has two consequences that deserve particular attention. The pre-breakup yields of protons, deuterons, and tritons are included in the double ratios used to determine the temperatures  $T_{\text{He}p d}$  and  $T_{\text{He}d t}$ . This violates the requirement of thermal and chemical equilibrium, which is the basic assumption of the method, and thus may shed doubt on the meaning of the consistency exhibited by Fig. 2. On the other hand, the quantum statistical model predicts that, in particular, the p/d ratio varies sufficiently slowly with temperature, such that the overall ratio will not be significantly affected by contributions from higher temperatures. The second point concerns the interpretation of the excitation energy that is obtained in a calorimetric measurement.

## 6 Excitation energy of primary spectators

Rather small fractions of the initial bombarding energy are imparted to the spectator nuclei in relativistic collisions. The actual amount of energy deposition can only be reconstructed from the exit-channel configuration which requires a complete

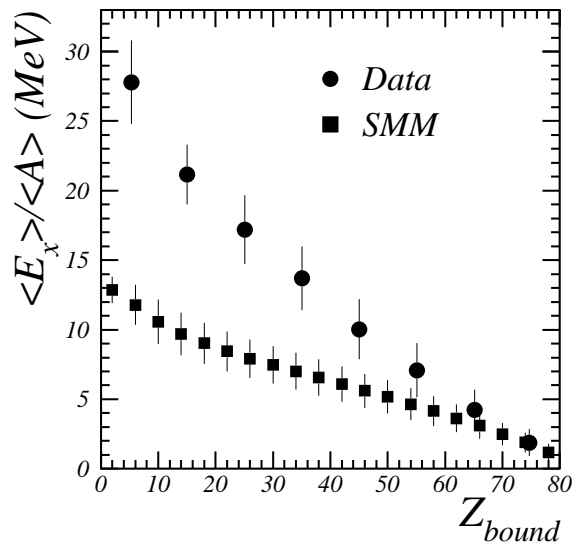


Figure 8: Reconstructed average excitation energy  $\langle E_x \rangle / \langle A \rangle$  of the decaying spectator system (circles) and mean excitation energy used in the calculations with the statistical multifragmentation model as a function of  $Z_{bound}$ .

knowledge of all decay products, including their atomic numbers, masses, and kinetic energies. A rather large fraction of it resides in the kinetic energies of the produced nucleons and in their separation energies.

For the analysis for the  $^{197}\text{Au} + ^{197}\text{Au}$  reaction at 600 MeV per nucleon, the data on neutron production measured with LAND were available [1, 26]. On the other hand, the hydrogen isotopes were not detected in this experiment and assumptions concerning their kinetic energies as well as the p/d/t intensity ratios and the overall  $N/Z$  ratio of the spectator had to be made. From the present experiment at 1000 MeV per nucleon, data on hydrogen emission from the target spectator source have been obtained. Together with the neutron data measured with LAND at the same bombarding energy in the previous experiment, a complete picture on light particle emission has become available for this reaction. It was found, in particular, that by adding a Coulomb component to the neutron kinetic energies, an assumption that had to be made previously, the proton kinetic energies are considerably underestimated (Fig. 7). Furthermore, the full analysis of neutron emission at three bombarding energies has revealed a significant dependence of the neutron kinetic energies on the bombarding energy. This phenomenon contrasts the universal properties of fragment production [20] but is clearly consistent with a pre-breakup component of nucleon emission exhibiting some residual memory of the initial stages of the reaction.

In Fig. 8 the result of the present analysis of the spectator energy and the excitation energies used for the calculations with the statistical multifragmentation

model are shown. In both cases, the values have increased considerably, compared to those reported previously [20]. The reasons have been given already. The masses  $A_0$  of the primary spectator systems, on the other hand, have remained the same as they consist mainly of the sum of the masses of the produced fragments of intermediate mass. They are in rather good agreement with the predictions of the geometrical participant-spectator model [36]. The maximum number of fragments, observed at  $Z_{bound} \approx 40$ , is associated with initial excitation energies of  $\langle E_x \rangle / \langle A \rangle \approx 12$  MeV and, according to the model calculations, with excitation energies of  $\langle E_x \rangle / \langle A \rangle \approx 6$  MeV in the equilibrium stage at breakup.

## 7 Summary

Breakup temperatures  $T_{\text{HeLi}}$ ,  $T_{\text{Hepd}}$ , and  $T_{\text{Hedt}}$  were measured for target spectators in  $^{197}\text{Au} + ^{197}\text{Au}$  collisions at 1000 MeV per nucleon. In these reactions multifragmentation is the dominant decay channel of the produced spectator systems over a wide range of excitation energy and mass. The corrections for sequential feeding of the ground-state yields, based on calculations with the quantum statistical model, resulted in mutually consistent values for the three temperature observables.

With decreasing  $Z_{bound}$ , the obtained temperatures increase from  $T = 4$  MeV for peripheral collisions to about 10 MeV for the most central collisions. Within the errors, these values are in good agreement with those measured previously with the ALADIN spectrometer for projectile spectators in the same reaction at 600 and 1000 MeV per nucleon. The agreement of the temperatures measured at 600 and 1000 MeV per nucleon confirms the expected invariance of the breakup temperature with the bombarding energy. It is consistent with the observed  $Z_{bound}$  scaling of the mean fragment multiplicities and charge correlations and supports the statistical interpretation of the multi-fragment decay of highly excited spectator nuclei.

The comparison with the results of calculations within the statistical multifragmentation model shows that a good simultaneous agreement for the charge partitions and for the breakup temperatures can be achieved. A necessary requirement for a consistent statistical description of the spectator fragmentation is thus fulfilled. The model results also suggest that the true source temperature varies slightly less, from  $T = 5$  MeV for peripheral to only about 9 MeV for the most central collisions, and stays rather constant  $T \approx 6$  MeV over the range of excitation energies where the maximum production of intermediate-mass fragments is observed.

The systematic behavior of the kinetic-energy spectra of light charged particles indicates contributions from light-particle emission prior to the final breakup stage. This is supported by the variation with bombarding energy of the kinetic-energy spectra of neutrons. A more quantitative understanding of the role of the pre-breakup processes will be essential for the interpretation of temperatures obtained from light-

particle yields as well as of the excitation energies obtained from calorimetric measurements of the spectator source.

## References

- [1] J. Pochodzalla *et al.*, Phys. Rev. Lett. 75 (1995) 1040.
- [2] T. Möhlenkamp *et al.*, *Proceedings of the XXXIII International Winter Meeting on Nuclear Physics*, Bormio, 1995, edited by I. Iori (Ricerca Scientifica ed Educazione Permanente, Milano, 1995), p. 383.
- [3] S. Albergo *et al.*, Il Nuovo Cimento 89A (1985) 1.
- [4] F. Gulminelli *et al.*, contribution to these Proceedings.
- [5] M.B. Tsang *et al.*, contribution to these Proceedings.
- [6] Z. Majka *et al.*, preprint 96-03, Texas A&M University, 1996.
- [7] X. Campi *et al.*, Phys. Lett. B385 (1996) 1.
- [8] S. Fritz *et al.*, contribution to these Proceedings, preprint nucl-ex/9704002.
- [9] J.B. Natowitz *et al.*, Phys. Rev. C52 (1995) R2322.
- [10] G. Papp and W. Nörenberg, preprint GSI-95-30 (1995); Proceedings of the International Workshop XXII, Hirschegg, 1994, edited by H. Feldmeier and W. Nörenberg (GSI, Darmstadt, 1994) p. 87.
- [11] L.G. Moretto *et al.*, Phys. Rev. Lett. 76 (1996) 2822.
- [12] D.H.E. Gross, Rep. Prog. Phys. 53 (1990) 605.
- [13] J.P. Bondorf *et al.*, Phys Rep. 257 (1995) 133.
- [14] H. Jaqaman *et al.*, Phys. Rev. C27 (1983) 2782.
- [15] M. Brack *et al.*, Phys. Rep. 123 (1985) 275.
- [16] S.J. Lee and A.Z. Mekjian, preprint nucl-th/9703012.
- [17] J.N. De *et al.*, preprint nucl-th/9703026.
- [18] J.A. Hauger *et al.*, Phys. Rev. Lett. 77 (1996) 235.
- [19] Y.-G. Ma *et al.*, Phys. Lett. B390 (1997) 41.
- [20] A. Schüttauf *et al.*, Nucl. Phys. A607 (1996) 457.
- [21] A.S. Botvina *et al.*, Nucl. Phys. A584 (1995) 737.

- [22] C. Schwarz *et al.*, contribution to these Proceedings, preprint nucl-ex/9704001.
- [23] D. Hahn and H. Stöcker, Nucl. Phys. A476 (1988) 718.
- [24] J. Konopka *et al.*, Phys. Rev. C50 (1994) 2085.
- [25] T. Möhlenkamp, PhD thesis, Universität Dresden, 1996, unpublished.
- [26] W. Trautmann *et al.*, *Proceedings of the XXXIII International Winter Meeting on Nuclear Physics*, Bormio, 1995, edited by I. Iori (Ricerca Scientifica ed Educazione Permanente, Milano, 1995), p. 372.
- [27] R. Botet and M. Ploszajczak, Phys. Lett. B312 (1993) 30; Acta Physica Polonica B25 (1994) 353.
- [28] J. Richert *et al.*, contribution to these Proceedings.
- [29] The projectile temperatures given in Fig. 3 are from Ref. [25]. At small  $Z_{bound}$ , i.e. at large excitation energies, they exceed those presented in Ref. [1] by 10 to 20%.
- [30] P. Désesquelles *et al.*, Nucl. Phys. A604 (1996) 183.
- [31] A.S. Botvina and I.N. Mishustin, Phys. Lett. B294 (1992) 23.
- [32] H.W. Barz *et al.*, Nucl. Phys. A561 (1993) 466.
- [33] P. Kreutz *et al.*, Nucl. Phys. A556 (1993) 672.
- [34] W.A. Friedman, Phys. Rev. C42 (1990) 667.
- [35] K. Kwiatkowski *et al.*, contribution to these Proceedings.
- [36] J. Gosset *et al.*, Phys. Rev. C16 (1977) 629.